Available online at www.sciencedirect.com

SCIENCE DIRECT®

Polymer 44 (2003) 5407–5421

polymer

www.elsevier.com/locate/polymer

The effect of hard segment ordering in copolyurethane elastomers obtained by using simultaneously two types of diisocyanates

C. Prisacariu[a], R.H. Olley[b,*], A.A. Caraculacu[a], D.C. Bassett[b], C. Martin[c]

[a]*The Romanian Academy's Institute of Macromolecular Chemistry 'Petru Poni', Aleea Grigore Ghica Voda, Nr. 41 A, 6600 Iasi, Romania*
[b]*J.J. Thomson Physical Laboratory, Polymer Science Centre, University of Reading, Whiteknights, Reading RG6 6AF, UK*
[c]*Department of Physics, School of Chemistry and Physics, Keele University, Staffordshire ST5 5BG, UK*

Received 28 February 2003; received in revised form 22 May 2003; accepted 3 June 2003

Abstract

A number of polyurethanes are synthesized, based on the novel diisocyanate 4,4′-dibenzyl diisocyanate (DBDI), the traditional 4,4′-methylene bis(phenyl isocyanate) (MDI), or combinations of these. Two equivalent series are prepared, one with hydroxyterminated poly(ethylene adipate) and one with poly(tetrahydrofuran) macrodiol. Mechanical measurements and X-ray crystallinity data are shown for the materials as prepared and after annealing. DBDI has a variable geometry, which allows crystallinity to develop, and leads to an increase in mechanical properties (tensile stress, ultimate strength stress, tear strength, hardness and strain energy): whereas the residual elongation is also dramatically increased. The general improvement in properties with DBDI is retained when both diisocyanates are included, especially when reacted together in a random fashion, rather than sequentially, in the prepolymer stage. Under these conditions, the residual elongation returns to that of a more conventional polyurethane, eliminating the major inconvenience derived from the high permanent deformability and high crystallinity which is undesirable for an elastomer. Scanning electron microscopy reveals coarse texture at the 10 μm level, and a finer texture at the 100 nm level which may be associated with the hard and soft polyurethane segments.

Keywords: Segmented polyurethanes; Diisocyanates; Thermomechanical behaviour

1. Introduction

The synthesis of polyurethane elastomers (PU) principally employs one of the limited number of commercially available diisocyanates, e.g. 4,4′- methylene bis(phenyl isocyanate) (MDI), tolylene-2,4-diisocyanate (TDI) or 1,5-naphthalene diisocyanate (NDI). Within this limitation, the large diversity of the known elastomers is achieved mainly by varying either the nature of polyhydroxyl components, namely the macrodiols and/or the polyol chain extender, or else in the case of polyurethane–ureas, the nature of amino chain extender. The present work reports research on PU elastomers obtained using a novel industrially available diisocyanate with a variable geometry, 4,4′-dibenzyl diisocyanate (DBDI) (Fig. 1(a)), whose synthesis was reported from our laboratory in 1959 [1]. As reported there, even if the structures of these diisocyanates differ only in the number of the methylene (CH_2) groups situated between the two aromatic rings bearing the isocyanate (NCO) groups in the para position, the properties of their polymers, especially the homopolyurethanes, are essentially different. Those with an even number of CH_2 groups situated between the aromatic rings are considerably higher melting than their odd-numbered counterparts [2].

DBDI was used both by itself and in combination with the more commonly available MDI (Fig. 1(b)). The literature is limited concerning mixtures of diisocyanates, which are specified only in a few patents [3].

As reported by ourselves [4,5] and Lyman [6], the MDI molecule introduces the rigid-Ph-CH_2-Ph- moiety in the elastomeric PU hard segments. In contrast when using DBDI, the specific-Ph-CH_2-CH_2-Ph- moiety introduces a variable geometry into the hard segments due to the possibility of internal rotation of this isocyanate around the $-CH_2-CH_2-$ ethylene bridge. This leads to the appearance of both 'syn' and 'anti' rotational conformations, which coexist in the DBDI based PU macromolecules. As a result, in this latter

---

* Corresponding author. Tel.: +44-118-931-8572; fax: +44-118-975-0203.

E-mail address: r.h.olley@reading.ac.uk (R.H. Olley).

0032-3861/03/$ - see front matter © 2003 Elsevier Ltd. All rights reserved.
doi:10.1016/S0032-3861(03)00489-0

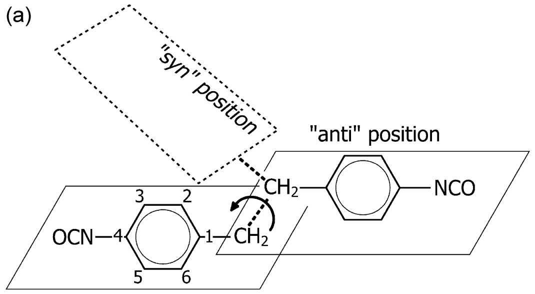

4,4'-dibenzyl diisocyanate (DBDI)

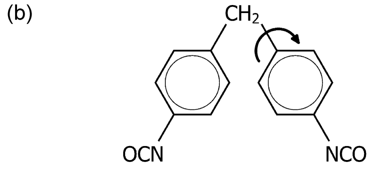

4,4'-diphenyl methane diisocyanate (MDI)

Fig. 1. Schematic of (a) DBDI and (b) MDI.

case the PU macromolecules can adopt a more compact packing which enhances significantly the ability to order in crystalline structures involving predominantly the anti form [2,5]. In the case of PU synthesized using mixtures of MDI and DBDI, it is expected to obtain copolyurethanes with novel properties. One of the initial questions is how to use these two monomers, the problem being to identify the eventual differences resulting when MDI and DBDI are introduced either concomitantly as a melt mixture or when they are inserted sequentially in the different stages of PU synthesis according to a multi step prepolymer technique.

It was shown [7] that PU with excellent mechanical properties were obtained when in the elastomer synthesis there was a small excess of diisocyanate relative to the total amount of the hydroxyl partners, namely macrodiol and extender. This diisocyanate excess has to compensate for some secondary NCO group consumption due to allophanate group formation, which perturbs the desired stoichiometric balance between the OH and NCO group concentrations necessary to achieve polymers with high molecular weights.

In concordance with this technique, a prepolymer obtained from the reaction between 1 mol of macrodiol, namely polyethylene adipate (PEA) or polytetrahydrofuran (PTHF), and 3–4 mol of diisocyanate, was reacted with a low molecular weight diol as extender in a quantity calculated so that there should remain theoretically an excess of unreacted NCO groups corresponding to an index $I = 110$ where:

$$I = (100 \times \mathrm{NCO}])/([\mathrm{OH}]_{\mathrm{M}} + [\mathrm{OH}]_{\mathrm{CE}})$$

where $[\mathrm{NCO}] =$ equivalents of NCO groups from the diisocyanate; $[\mathrm{OH}]_{\mathrm{M}} =$ equivalents of OH groups from the macrodiol; $[\mathrm{OH}]_{\mathrm{CE}} =$ equivalents of OH groups from the extender.

The value of $I = 110$ is sufficiently high so as to compensate the mentioned supplementary NCO groups consumption and to provide finally a variable free NCO group content (less than 0.0185 equiv. NCO/100 g PU). In accordance with this requirement, the quantity of bifunctional CE taken in reaction was: moles extender $= 0.455\,[\mathrm{NCO}] - 0.5[\mathrm{OH}]_{\mathrm{M}}$.

The so obtained active PU oligomer with terminated-NCO groups having a calculated M_{W} value of minimum 9–10,000 was further post-cured in the presence of air humidity at room temperature over two weeks. In these conditions the NCO excess groups in the 2 mm thick PU sheets were totally consumed leading mainly to new urea linkages besides the formation of some crosslinking allophanate bridges [7]. This situation is reflected by the decrease in the polymer solubility and achievement of maximum mechanical properties which will be discussed further.

2. Experimental

2.1. Synthesis of PU

2.1.1. Materials

The isocyanates were DBDI, which is an experimental product from the pilot plant (CIFC Savinesti, Romania) and was recrystallized twice from anhydrous cyclohexane mp 88–89 °C, and MDI from Aldrich. The macrodiols were hydroxy-terminated PEA $M_{\mathrm{W}} = 2000 \pm 50$ (PEA_{2000}), a commercial product from CIFC Savinesti, Romania, and hydroxy-terminated PTHF $M_{\mathrm{W}} = 2000 \pm 50$ (PTHF_{2000}) from BASF, while the extender was anhydrous ethylene glycol (EG) or 1,4 butanediol (BG) from Aldrich.

(a) *Homopolyurethanes* $[\mathrm{EG{-}MDI}]_n$, $[\mathrm{EG{-}DBDI}]_n$ and $[\mathrm{BG{-}DBDI}]_n$ was synthesized from 0.02 mol EG and 0.02 mol of MDI or DBDI and, respectively, from 0.02 mol BG and 0.02 mol DBDI. In all cases the reactions were performed in 20 ml of *N*-Methyl-2-pyrrolidinone (NMP) at 115 °C for 1.5 h. The clear viscous solutions were poured into water and the tough white polymer precipitate was washed with water and dried. The yields were essentially quantitative. Inherent viscosity at 25 °C was as follows: 1.15 (0.5% in DMF) for [EG–MDI]; 0.82 (0.5% in NMP with 2% LiCl) for [EG–DBDI] and 0.75 (0.5 % in NMP with 2% LiCl) for [BG–DBDI].

(b) *Copolyurethane elastomers from a single diisocyanate* $PU_{D\ PEA}$, $PU_{M\ PEA}$, $PU_{D\ PTHF}$ *and* $PU_{M\ PTHF}$ (Table 1). The following general procedure was undertaken: 100 g (0.05 mol) of macrodiol PEA or PTHF, respectively, was dehydrated under mixing at 110 °C and vacuum (<1 mm Hg) for 2 h. 52.8 g (0.2 mol) of DBDI for the

Table 1
PU stress–strain properties

Recipe	Type of PU structure[a] and moles		Hardness [Sh°A]	100% Tensile stress [MPa]	300% Tensile stress [MPa]	Ultimate strength stress, [Mpa]	Elongation at break [%]	Residual elongation [%]		Tear strength [N/mm]
								(a)	(b)	
1. $PU_{C1\ PEA}$	EG–PEA–(DBDI–MDI) (2.64:1:2:2)	I	98	11.04	25.3	48.7	450	24	20	79.5
		A	96	6.29	13	45.6	575	25	–	–
2. $PU_{C2\ PEA}$	EG–(PEA–DBDI)–MDI (2.64:1:2:2)	I	94	9.3	24.7	41.6	375	60	50	76.7
3. $PU_{C3\ PEA}$	EG–(PEA–MDI)–DBDI (2.64:1:2:2)	I	99	11.3	24	30.3	350	50	40	98.2
4. $PU_{C1\ PTHF}$	EG–PTHF–(DBDI–MDI) (2.64:1:2:2)	I	98	11	24.3	24.3	300	5	3	53.4
		A	96	8.8	14.9	33.6	450	–	30	–
5. $PU_{C2\ PTHF}$	EG–(PTHF–DBDI)–MDI (2.64:1:2:2)	I	99	10.3	21.3	21.3	300	20	15	71.7
		A	95	7.7	13.8	34.2	450	–	80	–
6. $PU_{C3\ PTHF}$	EG–(PTHF–MDI)–DBDI (2.64:1:2:2)	I	100	11.5	–	18.9	250	10	7.5	84.8
		A	98	11.3	15.7	33.9	475	–	70	–
7. $PU_{D\ PEA}$	EG–PEA–DBDI (2.64:1:4)	I	98	15.8	19.5	33.7	525	155	155	116
			96	12.8	17.3	27.7	600	240	–	–
8. $PU_{M\ PEA}$	EG–PEA–MDI (2.64:1:4)	I	92	8.1	22	47	425	45	35	99.5
9. $PU_{D\ PTHF}$	EG–PTHF–DBDI (2.64:1:4)	I	96	13.6	14.8	27.6	525	160	160	116.2
10. $PU_{M\ PTHF}$	EG–PTHF–MDI (2.64:1:4)	I	94	8.7	21.4	21.4	300	10	10	51.8

I—initially; A—after annealing at 160 °C for 30 min; (a)—immediate residual elongation; (b)—residual elongation after 1 week.

[a] The structure is shortly represented by the nature and the molar ratios of the monomers used in synthesis. A more exact representation of the structure is given in the schematic of PU synthesis.

PU_D type or, respectively, 50 g (0.2 mol) of MDI in the case of PU_M type of elastomer, was added at once under intense mixing to the anhydrous macrodiol, and vacuum was restored. After 30 min of mixing under vacuum at 100 °C the temperature was reduced to 90 °C and vacuum was removed. This gave a prepolymer with final NCO groups in mixture with excess of isocyanate. Next, 8.18 g (0.1318 mol) EG extender were added at once under rapid stirring. The mixing was continued for maximum 30–40 s.

The 'pot life' of the mixture was between 3 and 10 min depending on the PU structure. During this time the liquid mixture was cast onto closed teflonated mouldings preheated at 90 °C so as to avoid the influence of air humidity during the cure process. In the case of open moulding the presence of air on the upper sheet surface usually leads to some uncontrolled and inhomogeneous modifications of the mechanical properties. For the cure process the closed mouldings were maintained after casting at 110 °C for 24 h. After an additional 24 h at room temperature, the polymeric sheets representing an active PU oligomer with NCO final groups, were demoulded. The mechanical properties were measured after holding under ambient conditions for at least two weeks, during which period the active PU oligomers were transformed into the final elastomers. This period of time was necessary to finish the postcure process [7] in the case of PU sheets 0.3–2 mm thick when the remaining amount of NCO excess group was consumed mainly through the reaction with the air humidity, leading to new urea group linkages.

(c) *C1 series*. Copolyurethane elastomers from two diisocyanates randomly distributed $PU_{C1\ PEA}$ and $PU_{C1\ PTHF}$ (Table 1) were synthesized starting from PEA or from PTHF as in the case (b). The only difference was that in both cases in the prepolymer synthesis there was used a melt mixture of 26.4 g (0.1 mol) of DBDI with 25 g (0.1 mol) of MDI which was introduced into the anhydrous polyol at once. The following synthesis step e.g. the chain extension, curing and postcuring were performed similarly as in the case of general procedure (b).

(d) *C2 and C3 series*. Copolyurethane elastomers from two diisocyanates with selective diisocyanate distribution $PU_{C2\ PEA}$ and $PU_{C2\ PTHF}$ besides $PU_{C3\ PEA}$ and $PU_{C3\ PTHF}$ (Table 1) In this case, the polyaddition process involved a prepolymer synthesis in two steps. Thus for $PU_{C2\ PEA}$ and $PU_{C2\ PTHF}$, the first prepolymer was obtained by adding in the first step 26.4 g (0.1 mol) of DBDI in 100 g (0.05 mol) of anhydrous PEA or PTHF, respectively, under similar conditions as for the synthesis of the single prepolymer step technique as mentioned at (b). Into the prepolymer obtained, 25 g (0.1 mol) of MDI were dissolved. After 30 min of mixing the following synthesis steps e.g. chain extension, cure and postcure process performed also as in the case (b). The synthesis of $PU_{C3\ PEA}$ and $PU_{C3\ PTHF}$ involved also a two step prepolymer synthesis similar as for the $PU_{C2\ PEA}$ and $PU_{C2\ PTHF}$ with the only difference that the first introduced diisocyanate was 0.1 mol of MDI followed by dissolution of 0.1 mol of DBDI in the prepolymer. The following synthesis step e.g. the chain extension, curing and postcuring, were performed similarly as in the case of general procedure (b).

2.2. Etching

Etching of specimens for microscopy was performed according to the recipe developed for polyetheretherketone [8]. The reagent consisted of a solution of 1.6 g of potassium permanganate which was first dissolved with continuous stirring in 64 ml of orthophosphoric acid (Merck 85% reagent). When dissolution was complete, 16 ml of water was added to give the working reagent. Specimens were shaken in this for 45 min, after which an equal volume of hydrogen peroxide, diluted to give 3% in water, was added to stop the reaction. Specimens were then washed with several changes of distilled water, and dried.

2.3. Scanning electron microscopy

Scanning Electron Microscopy (SEM) was performed on the outer surface of the original cast sheets prepared as presented in the previous section, and after etching. Specimens were coated with a sputtered film of gold to prevent charging, and were tilted at 45° in the specimen chamber to improve contrast [9].

2.4. 300% Tensile stress and strength stress determination

300% Tensile stress and the strength stress determinations were made in accordance with standard procedures from the stress–strain curve data of simple uniaxial tension. The specimens for the testing were cut from films using dimension given in ASTM D1708, i.e. a dumbbell-shaped specimen with a gauge length of 20 mm, a width of 58 mm, and 0.3 up to 2 mm thickness. The stress–strain data on these specimens presented here were taken by using a Universal Instron Testing Machine at room temperature ($T = 25$ °C).

2.5. WAXD measurements

A. Wide-angle X-ray scattering (WAXD) patterns shown in Fig. 5(a)–(f), were collected at the European Synchrotron Radiation Facility (ESRF), Grenoble. The data were collected on the Microfocus Beamline ID13 which provided a 5 μm diameter beam. This beamline is based on an undulator in a low-β section of the storage ring and is optimized for microfocus diffraction. Typically, for WAXD experiments, a liquid nitrogen cooled Si (111) channel-cut monochromator and ellipsoidal mirror were used to focus the X-ray beam to a size of about 20 μm × 20 μm at the sample position to give a flux density of about 6×10^9 photons $s - ^1$ $\mu m - ^2$ (at an energy of 13 keV [see the ESRF website: http://www.esrf.fr/exp_facilities/ID13/handbook/capillary.htm]). The photon energy for these experiments was 12.9 keV. The schematic is shown in Fig. 2.

The PU film samples were held on a sample holder, placed in the sample position normal to the incident beam and diffraction data collected in transmission mode. Exposure times were 20 s and data were collected by a 16-bit MAR–CCD detector. The detector had a 130 mm diameter entrance window and was used in 1024 × 1024 pixels mode. A separate 'empty camera' exposure was taken for background subtraction purposes [10].

B. WAXD measurements shown in Figs. 3 and 4 were measured by a TUR M62 diffractometer on films, using Cu Kα radiation (36 kV, 20 mA).

2.6. DSC Measurements

Differential scanning calorimetry (DSC) determinations were performed by a Mettler TA instrument DSC 12E with a heating rate of 20 °C/min, in nitrogen.

2.7. Thermomechanical measurements

The thermomechanical measurements were performed on a home-made instrument as previously reported [11].

3. Results and discussion

3.1. Synthesis

In the first step of our study presented in this paper, we have used the generally employed method of PU synthesis in the melt, namely the prepolymer route which first incorporates the soft segments followed by a reaction with a chain extender to build up the hard segments. The materials are subsequently postcured with air humidity, which consumes all of the isocyanate excess situated on the ends of the intermediary formed active PU oligomer, thereby leading to an additional degree of urea group formation [7]. In our case this refers to a PU synthesized by using a 1 mol of macrodiol-4 mol diisocyanate-2.64 mol chain extender system, so to obtain a small isocyanate group excess ($I = 110$) situated at the ends of the above active PU oligomer.

The two parallel series started with one or other of two hydroxy-terminated macrodiols with $\bar{M} = 2000 \pm 50$ as follows: a polyester type-PEA (PEA_{2000}) or a polyether type-PTHF ($PTHF_{2000}$).

For those PU elastomers containing simultaneously two different diisocyanates, 1 mol of macrodiol was reacted in the following different ways with 2 mol of MDI and 2 mol of DBDI.

- PU_{C1}: Single step prepolymer synthesis which uses a melt mixture of the two isocyanates (MDI and DBDI isocyanates). In this case, the two different diisocyanates are inserted more or less randomly into the prepolymer and in the resulting full polymer.
- PU_{C2}: A two-step prepolymer synthesis where two moles of DBDI is first reacted with one mole of macrodiol, followed by addition of MDI.
- PU_{C3}: A two-step prepolymer synthesis where two moles of MDI is firstly reacted with one mole of macrodiol, followed by addition of DBDI.

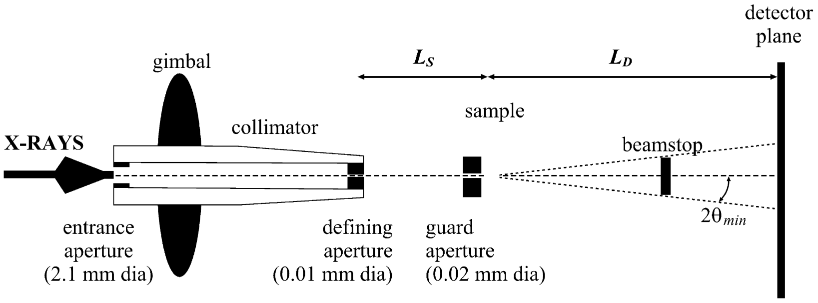

Fig. 2. Schematic illustration of the setup used to collect the WAXD data. For the WAXD experiments described the distance L_D was set to about 180 mm. The collimator exit aperture was 5 μm diameter and the beamstop was approximately 300 μm.

In all cases, active oligomers are obtained with final NCO groups having a calculated molecular weight of about 8900. Finally the so-obtained different prepolymers were reacted with 2.64 mol of chain extender which was in all cases EG. There were adopted three different modes of prepolymer synthesis leading to three different active PU oligomers.

The equations are displayed in Scheme 1. We should note that these equations only display a global average picture, in reality, under these conditions the number of species of molecules which appear during the prepolymer synthesis is higher due to the statistical probability of the competitive reaction of unreacted macrodiol molecules with the newly formed macrodiisocyanate and remaining initial diisocyanate, as has been found with low molecular reactant partners [12]. The statistics are especially simple in the condition of quasi-equal reactivity of both functional groups on each difunctional species, before and after the first functional group has reacted. In the case of the macrodiol the reactivity of the two final OH groups should be equal, but the reactivity of the two OH groups of EG toward a monoisocyanate (phenyl isocyanate) was found not to be equal ($k_1/k_2 = 2.59$ [13]): this difference is determined by the simultaneous presence of intramolecular hydrogen bonding of the two EG OH groups [13,14]. In regard to NCO groups, the reactivity is expected to be the same for M and D, from a model reaction in which it was found that the first reaction rate constant of MDI with *n*-butanol is practically equal to that of DBDI [12]. With or without differences in the reaction rates, the quantity of the free diisocyanate in prepolymer is somewhat higher than that calculated and the mixture would also contain molecules of prepolymer as that of M* ∧∧∧ M ∧∧∧ M*, respectively, D* ∧∧∧ D ∧∧∧ D* or even longer.

In principle, in order to obtain a more regular structure one could adopt an inverse procedure using a special alternating step by step laboratory synthesis of the desired hard segments. In this procedure, the reactants would be taken in succession one by one in a large excess followed in every stage by a careful purification of the intermediate reactive species. However, due to the high melting point of the intermediate products, this procedure can be used only in the solution method. For practical reasons we resort in this work to the more usual applicable and less laborious procedure in the melt.

The properties of these copolyurethanes were compared to the properties of the respective homopolyurethane elastomers—either (PU_D) or (PU_M):

$$[(GD)_3 \wedge\wedge\wedge\wedge\wedge\ D]_n \text{ or } [(GM)_3 \wedge\wedge\wedge\wedge\wedge\ M]_n$$

As a reference for the behaviour of the different types of PU hard segments which occur in the below presented copolymer, other types of PU models were also synthesized using the simple reaction between the single diisocyanate, MDI or DBDI, and EG in a 1:1 molar ratio, as $[EG-MDI]_n$, $[EG-DBDI]_n$ and $[BG-MDI]_n$,. Also other simpler copolyurethane elastomers derived from a single diisocyanate, DBDI or MDI and PEA or PTHF, using in all the cases EG as extender were synthesized. Thus, the $PU_{D\ PEA}$, $PU_{M\ PEA}$,

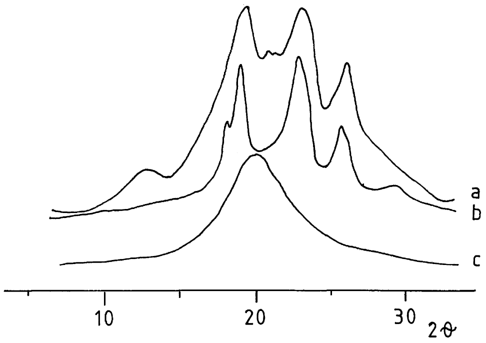

Fig. 3. WAXD of polyurethanes containing only hard segments: (a) $[BG-DBDI]_n$; (b) $[EG-DBDI]_n$; (c) $[EG-MDI]_n$.

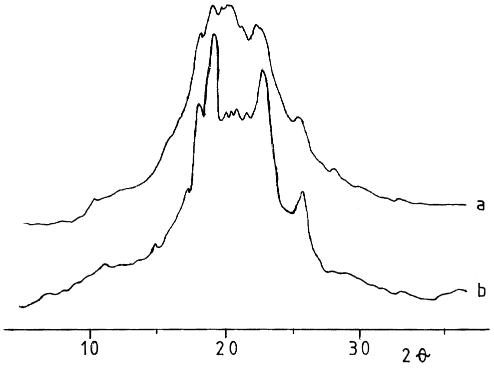

Fig. 4. WAXD of polyurethanes: (a) $PU_{C1\ PEA}$ and (b) $PU_{D\ PEA}$.

Synthesis of PU$_{C1}$ type active oligomer

HO ʌʌʌʌʌ OH + (2 MDI + 2DBDI) → U* ʌʌʌʌʌ U* + 2 (x MDI + y DBDI)
melt mixture → prepolymer U

[U* ʌʌʌʌʌ U* + 2 (x MDI + y DBDI)] + 2.64 EG → OCN U*[G (UG)$_{1.64}$ U ʌʌʌʌʌ U]$_{2.77}$ NCO

Synthesis of PU$_{C2}$ type active oligomer

HO ʌʌʌʌʌ OH + 2 DBDI → D* ʌʌʌʌʌ D*
prepolymer (D)

[D* ʌʌʌʌʌ D* + 2 MDI] + 2.64 EG → OCN M*[G (MG)$_{1.64}$ D ʌʌʌʌʌ D]$_{2.77}$ NCO

Synthesis of PU$_{C3}$ type active oligomer

HO ʌʌʌʌʌ OH + 2 MDI → M* ʌʌʌʌʌ M*
prepolymer (M)

[M* ʌʌʌʌʌ M* + 2 DBDI] + 2.64 EG → OCN D*[G (DG)$_{1.64}$ M ʌʌʌʌʌ M]$_{2.77}$ NCO

where : ʌʌʌʌʌ = macrodiol chain G = extender chain [-(CH$_2$)$_2$-]
M* and D* = monourethane – isocyanate sequence derived from monoreacted MDI and respectively DBDI;
M and D = diurethane sequence derived from bireacted MDI and respectively DBDI;
U* and U = mono and respectively diurethane sequence derived from either randomly mono and bireacted MDI or DBDI.
x + y = 1

Scheme 1. Active PU oligomer synthesis from two diisocyanates.

PU$_{D\ PTHF}$ and PU$_{M\ PTHF}$ copolyurethanes were obtained and used as additional models.

3.2. Crystallinity

The excellent properties of PU originate mainly from their special tendency to form discrete regions in which the hard segments made up by diisocyanate and extender tend to self-associate in separate microdomains. Sometimes these associations are ordered to such an extent that they can be evidenced by their characteristic X-ray diffraction. A good way to study this process is to take into account as a simple model substance the homopolyurethanes [EG–MDI]$_n$ or [EG–DBDI]$_n$, which reproduces the structure of the hard segments from the different complex copolyurethane elastomers. Fig. 3 displays some typical WAXD curves. The [EG–DBDI]$_n$ is a polymer with a high tendency to crystallize (Fig. 3(b)), both in terms of quantity of crystalline material and the definition of the X-ray reflections. This behaviour is paralleled by the self-separation of crystalline polymer from its solution with time [2]. The [EG–MDI]n (Fig. 3(c)) shows only a single broad peak, rather narrower than might be expected for an amorphous halo, suggesting rather a loose association of molecular chains. This material does not crystallize from solution [2].

This capacity for crystallization is characteristic not only for the [EG–DBDI]$_n$ structure, but also for similar DBDI based materials based on 1,4-butanediol, as in the case of [BG–DBDI]$_n$ in Fig. 3(a). An extender with an even number of methylene units should allow the diisocyanate molecule to assume an almost linear 'anti' conformation, so these materials should exhibit an 'odd–even' variation in their ability to crystallize as observed in similar cases [2].

The X-ray diffraction patterns of Fig. 4 show that the crystallizability of DBDI based material largely remains even after the inclusion of the soft segments (in this case PEA, Fig. 4(b)); this indicates the appearance of more or less complete phase separation associated with the formation of discrete crystalline hard domains.

The presence of these structures induces a special mechanical behaviour in the elastomers. Due to the disordered orientation of these domains in the polymer matrix the materials appear initially isotropic on the macroscale but when subjecting the polymer to stretching, these microdomains tend to orient in parallel, maintaining to some extent the so obtained anisotropy even after removing the stress. As a result some enhanced residual elongation was evident and the chain orientation was substantially confirmed by using a polarizing optical microscope. Supplementary studies on this subject were performed employing IR dichroism [15].

The crystallinity is, however, considerably reduced with the incorporation of MDI, of which the example of PU$_{C1\ PEA}$ is presented in Fig. 4(a). In all the PU containing two diisocyanates, namely the PU$_{C1}$, PU$_{C2}$ and PU$_{C3}$ types, with either of the soft segments PEA or PTHF, the X-ray diffraction patterns show that the crystallinity decreases significantly relative to those PU containing only DBDI (PU$_D$) indicating a decrease of the hard segments ordering.

To compare more critically the different routes of copolymerization PU$_{C1}$, PU$_{C2}$ and PU$_{C3}$, and their effect on the hard segment ordering, a further series of WAXD data was collected at the ESRF, Grenoble.

These results major on the PTHF series of materials. With these also, when employing the PU synthesis with mixtures of DBDI and MDI, the crystallinity is decreased relative to the unmixed PU_D polyurethane, but it is very apparent from Fig. 5 that the degree to which crystallinity is depressed depends critically on the synthesis route. Clearly, the sharp peaks associated with DBDI decrease in the order:

$$PU_D > PU_{C3} > PU_{C1} > PU_{C2} > PU_M$$

corresponding to introduction of DBDI as follows:

> total polymer:: hard segments:: mixed:: soft segments:: none.

Surprisingly, in the case of $PU_{C2\ PTHF}$ when MDI is introduced in the second stage, there is still a suggestion of the DBDI peaks, but the peak '2' is being replaced by the broad peak 2 associated with MDI only. This correlates with an observed practical total loss of crystallinity (Table 2).

Note that χ_c is not a calibrated absolute crystallinity. It represents a crystallinity index and has validity for comparative purposes only in this context.

It is to be noted that the substitution of the soft segment from PTHF to PEA does not change the above mentioned conclusions. The WAXD patterns of corresponding pairs based on PEA or PTHF are similar in all cases.

3.3. DSC measurements

Thermal analysis shows evidence of profound differences in structure brought about by changing the copolymeric ordering, both for the PEA series (Fig. 6) and the PTHF series (Fig. 7).

In addition to the copolymers, in order to obtain a better attribution of the DSC maxima, both simple model macromolecule models (homopolymers) were used which reproduce parts of the copolymer chain as hard sequence $(EG–MDI)_n$ and $(EG–DBDI)_n$ and also simple elastomers with only one diisocyanate, namely PU_M and PU_D in their PEA and PTHF varieties.

DSC maxima in the region between 20 and 150 °C are characteristic mainly of ordered soft segment structure as observed in the case of stretched $PU_{D\ PTHF}$ model when a small maximum at 50 °C reveals crystallization of the PTHF segments, which persists after removing the stress (Fig. 7(e), curve 2). Such a tendency was observed also in many other PU [15]. As observed all the PU obtained by using mixtures of diisocyanates ($PU_{C1\ PEA}$ and $PU_{C1\ PTHF}$) do not display such maxima.

The region 150–230 °C characteristic of a mesophase transformation is very sensitive to the changes in the copolymeric ordering. So, the mesophase in which there are involved MDI and PEA soft segments, displays two maxima at 195° and at 217 °C (Fig. 6(d)), whereas when using DBDI and PEA there do not appear clear significant similar interactions (Fig. 6(e)). A comparable situation appeared in the PTHF series, albeit with a small shift toward lower temperatures at 185° and at 206 °C, respectively (Fig. 7(d)), indicating that the interaction of the (MDI-EG) hard segments with PTHF is somewhat weaker. This situation is probably due to the weaker NH···O hydrogen bonding in PTHF relative to NH···O=C < in PEA, where the carbonyl ester group is involved.

As shown in Figs. 6 and 7 (solid and dotted lines), all the copolyurethanes are sensitive to supplementary thermal treatments. After annealing at 160° for 30 min all the mesophase interactions tend to diminish and as will be shown in a subsequent section the mechanical properties are influenced significantly.

DSC measurements also confirm the fact that in the two step synthesis the later introduced diisocyanate determines the preponderant nature of the hard segments. Thus the maximum characteristic for the $(EG–MDI)_n$ homopolyurethane at 246 °C (Fig. 6(f)) can be found again in the range of 240–248 °C. This is the case for $PU_{M\ PEA}$ at 248 °C (Fig. 6(d)), $PU_{C2\ PEA}$ at 244 °C (Fig. 6(b)) and $PU_{C2\ PTHF}$ at 240 °C (Fig. 7(b)), respectively. This maximum is also visible, but in smaller measure, when MDI and DBDI were introduced as a mixture in the reaction as for $PU_{C1\ PTHF}$ at 238 °C (Fig. 7(c)).

A special situation appears in the case of DBDI when the -$[EG–DBDI]_n$ segments display an exceptional tendency to crystallize and to self associate (Fig. 3(b)). The respective homopolymer EG–DBDI presents hard self interactions characterized by a high endotherm temperature maximum at 287 °C (Fig. 6(g)). This maximum can be found again also in the $PU_{D\ PEA}$, at 284 °C (Fig. 6(e)). The peculiar behaviour of the EG–DBDI sequence is revealed also when studying the DSC curves of the simple elastomer type $PU_{D\ PTHF}$ (Fig. 7(e)). In this case there is a lower tendency of the ether group to participate in hydrogen bond association with the urethane EG–DBDI segments than that observed with ester groups ($PU_{D\ PEA}$). As a result, during the PU synthesis in melt, in the last step of the process related to the EG–DBDI segment appearance, the melt viscosity increases quite quickly and part of the formed EG–DBDI segments does not have time to segregate in self associations, remaining in a dissolved state in the vitrified polymer matrix (the maximum characteristic for EG–DBDI at 287 °C does not appear anymore).

During the DSC measurements, once the temperature is raised sufficiently the polymer matrix becomes more mobile and allows the EG–DBDI segments to move and crystallize in self-associations. The crystallization is evidenced by the exothermic maxima appearing at 225 °C (Fig. 7(e), curve1-see also 230 °C in Fig. 7(c)-solid line, characteristic of $PU_{C3\ PTHF}$ which also has segments of the same type). On repeating 3 times the DSC scanning of $PU_{D\ PTHF}$ till 250 °C this exotherm maximum disappears completely and there is a significant increase in the EG–DBDI characteristic crystalline maximum at 277 °C (Fig. 7(e), curve 4).

Interpretation of the DSC curves above 250 °C in the

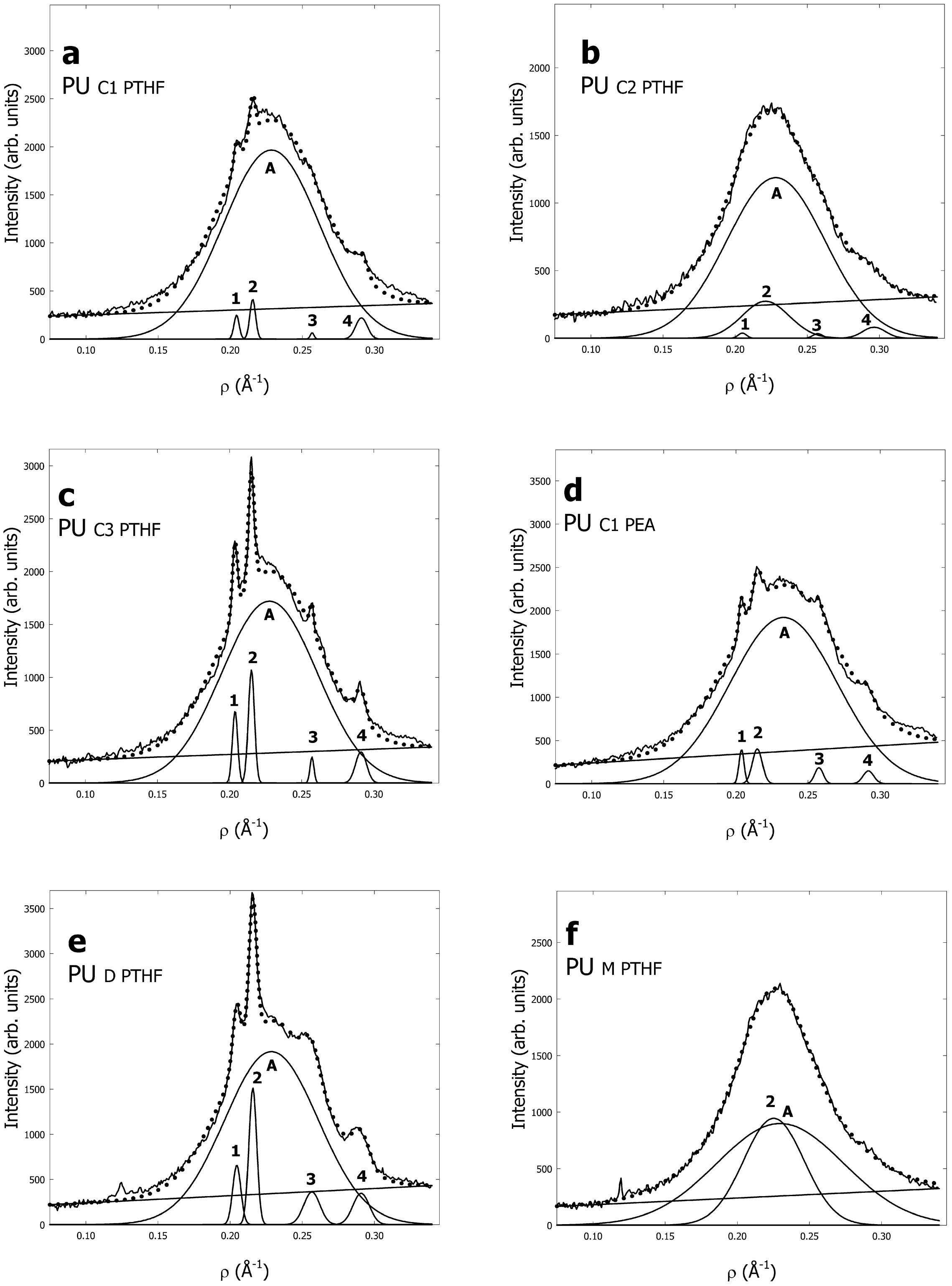

Fig. 5. (a) WAXD pattern collected from sample $PU_{C1\ PTHF}$ showing the separation of the scattering into crystalline and amorphous components; (b)WAXD pattern collected from sample $PU_{C2\ PTHF}$ showing the separation of scattering components. Here, all the peaks are broad, indicating an amorphous structure; (c) WAXD pattern collected from sample $PU_{C3\ PTHF}$ showing the separation of the scattering into crystalline and amorphous components; (d) WAXD pattern collected from sample $PU_{C1\ PEA}$; (e) WAXD pattern collected from sample $PU_{D\ PTHF}$ showing the separation of the scattering into crystalline and amorphous components; (f) WAXD pattern collected from the sample $PU_{M\ PTHF}$.

Table 2
Results for crystallinity index, χ_c. I_c, I_a and I_{tot} represents the measured integrated intensities for the crystalline, amorphous and total scattering components, respectively, in arbitrary units

Sample No.	I_c	I_a	I_{tot}	χ_c
$PU_{C1\ PTHF}$	5.6	164.6	170.2	0.03
$PU_{C2\ PTHF}$	–	–	–	–
$PU_{C3\ PTHF}$	12.5	142.9	155.4	0.08
$PU_{C1\ PEA}$	8.0	178.9	186.9	0.04
$PU_{D\ PTHF}$	24.9	155.7	180.6	0.14
$PU_{M\ PTHF}$	–	–	–	–

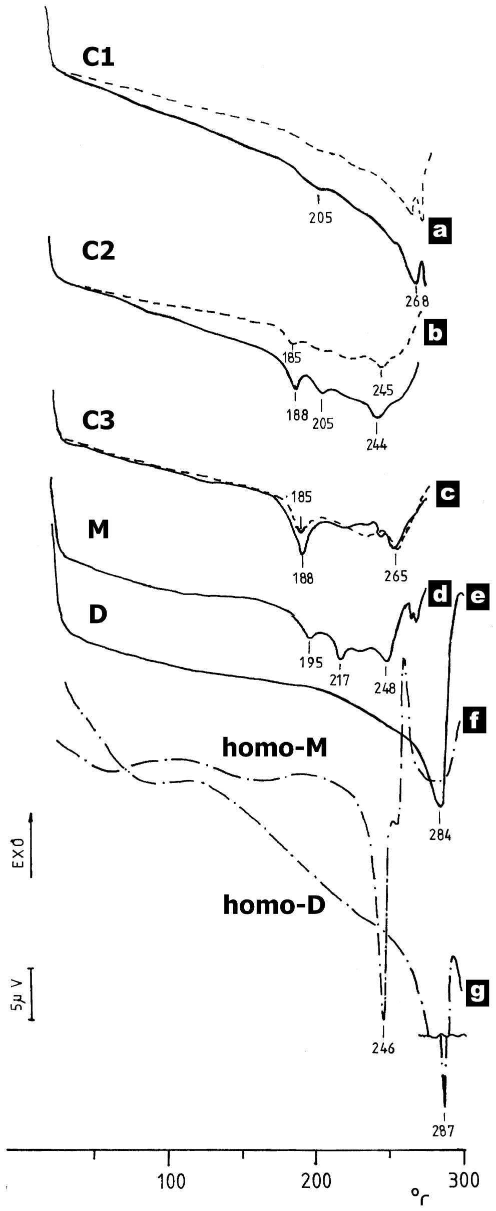

Fig. 6. DSC curves of copolyurethanes based on PEA: (a) $PU_{C1\ PEA}$—9.9 mg (I), 8.0 mg (A); (b) $PU_{C2\ PEA}$—8.1 mg (i), 8.0 mg (A); (c) $PU_{C3\ PEA}$—9.9 mg (I), 7.8 mg (A); (d) $PU_{M\ PEA}$-9.9 mg (I); (e) $PU_{D\ PEA}$—2.2 mg (i) (A); (f) homopolyurethane-$[EG-MDI]_n$—3.6 mg (A); (g) homopolyurethane-$[EG-DBDI]_n$—4.2 mg (A); solid lines-initial samples (I); dotted lines-after annealing (A) at 160 °C for 30 min.

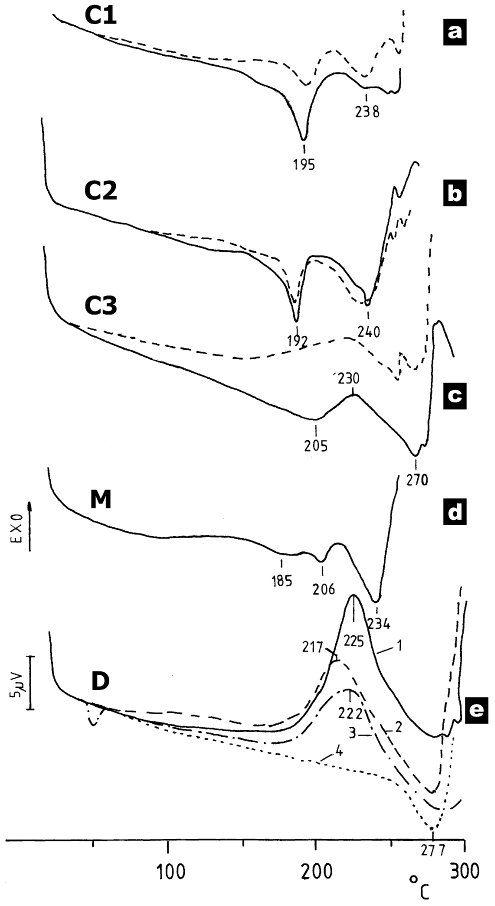

Fig. 7. DSC curves of copolyurethanes based on PTHF: (a) $PU_{C3\ PTHF}$—12.6 mg (I), 13.5 mg (A); (b) $PU_{C2\ PTHF}$—13.0 mg (I), 11 mg (A); (c) $PU_{C1\ PTHF}$—11.7 mg (I), 11.9 mg (A); (d) $PU_{M\ PTHF}$ 10.7 mg (A); (e) $PU_{D\ PTHF}$ (1)—9.4 mg initially; (2) 9.4 mg (after stretching till rupture); (3) 9.6 mg after annealing at 180 °C for 1 h; (4) 8 mg after annealing on repeating 3 times the DSC scanning of the sample till 250 °C.

case of the polymers containing EG–DBDI segments should be made with prudence, due to the fact that as we found on thermogravimetric analysis, all of the studied PU begin to decompose at about 250 °C and at about 275 °C their loss in weight represents approx. 5%. So in this region some variation in the DSC curves is more or less brought about by the incipient degradation thermal effects.

Fortunately, a similar partial crystallization effect as mentioned before can be obtained on the same polymer at lower temperatures (180 °C, 1 h) (Fig. 7(e), curve 3), and also at normal temperatures as a result of the polymer stretching (Fig. 7(e), curve2). Evidently, in these situations the thermal degradation process cannot be involved.

With regard to the main view of this work, namely the effect of different orderings in copolyurethanes based on two isocyanates, the DSC curves exhibit significant differences depending on the copolyurethane ordering. The DSC mesophase maxima are more pronounced in the step-by-step prepolymer synthesis and are governed mainly by the type of the last introduced diisocyanate which is responsible for the hard segment EG–MDI or EG–DBDI

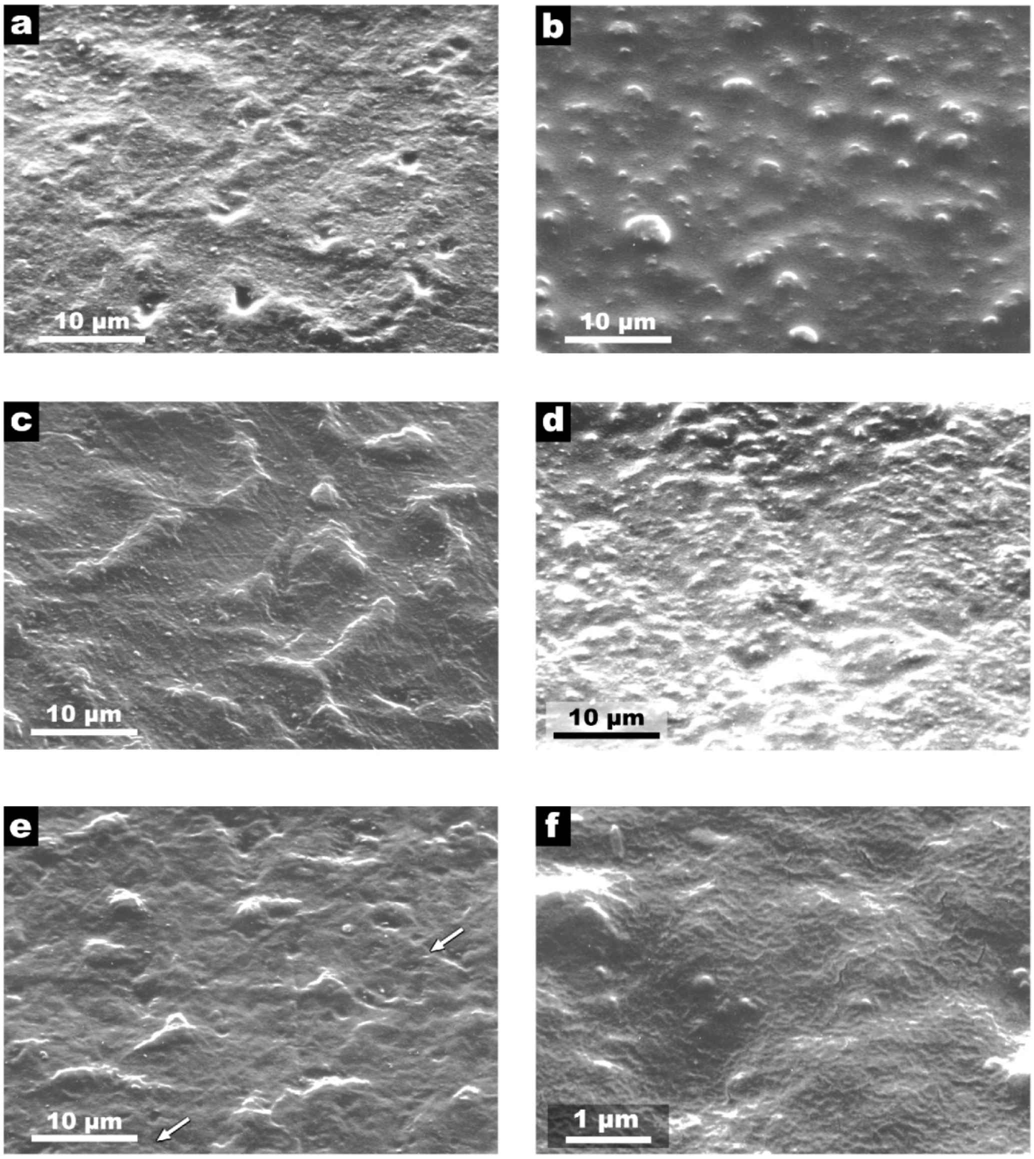

Fig. 8. SEM at medium magnification of (a) 4: $PU_{C1\ PTHF}$ (b) 5: $PU_{C2\ PTHF}$ (c) 6: $PU_{C3\ PTHF}$ (d) 9: $PU_{D\ PTHF}$ (e) 10: $PU_{M\ PTHF}$ (f) SEM at higher magnification showing fine texture of $PU_{M\ PTHF}$.

formation, respectively. In the one step prepolymer procedure when the two MDI and DBDI isocyanates are introduced at once, the copolyurethane displays a more irregular structure and no such evident mesophase DSC maxima are revealed.

3.4. Morphology

The surface structure of these materials contains features at two levels. All the materials display a relatively coarse structure on the 10 μm scale, but which varies considerably from material to material. This is shown in Fig. 8(a)–(f), for the PTHF materials. Of these, (4, 5, 6, 9 and 10 in Table 1), $PU_{C3\ PTHF}$ has the coarsest structure (Fig. 8(c)) while $PU_{M\ PTHF}$ has the finest (Fig. 8(e)). The materials which display X-ray crystallinity (4, 6 and 9, parts (a), (c) and (d) of Fig. 8) tend to give a rougher surface morphology than those, which do not (5 and 10, parts b and e). The specimens also show variations in topography such as long scratch marks which derive from the PTFE plates against which the sheets were moulded, although we have avoided showing regions where these obscure the characteristic texture of the materials.

There is also a finer texture of scale less than 100 nm, which may correspond to segregation of the two different chemical parts, namely the hard segment and soft segment. This is only observed by operating the SEM at higher accelerating voltage and smaller spot size, as in Fig. 8(f). Shown here is $PU_{M\ PTHF}$, but finer structure is present in the other materials also. This, however, was not intensively

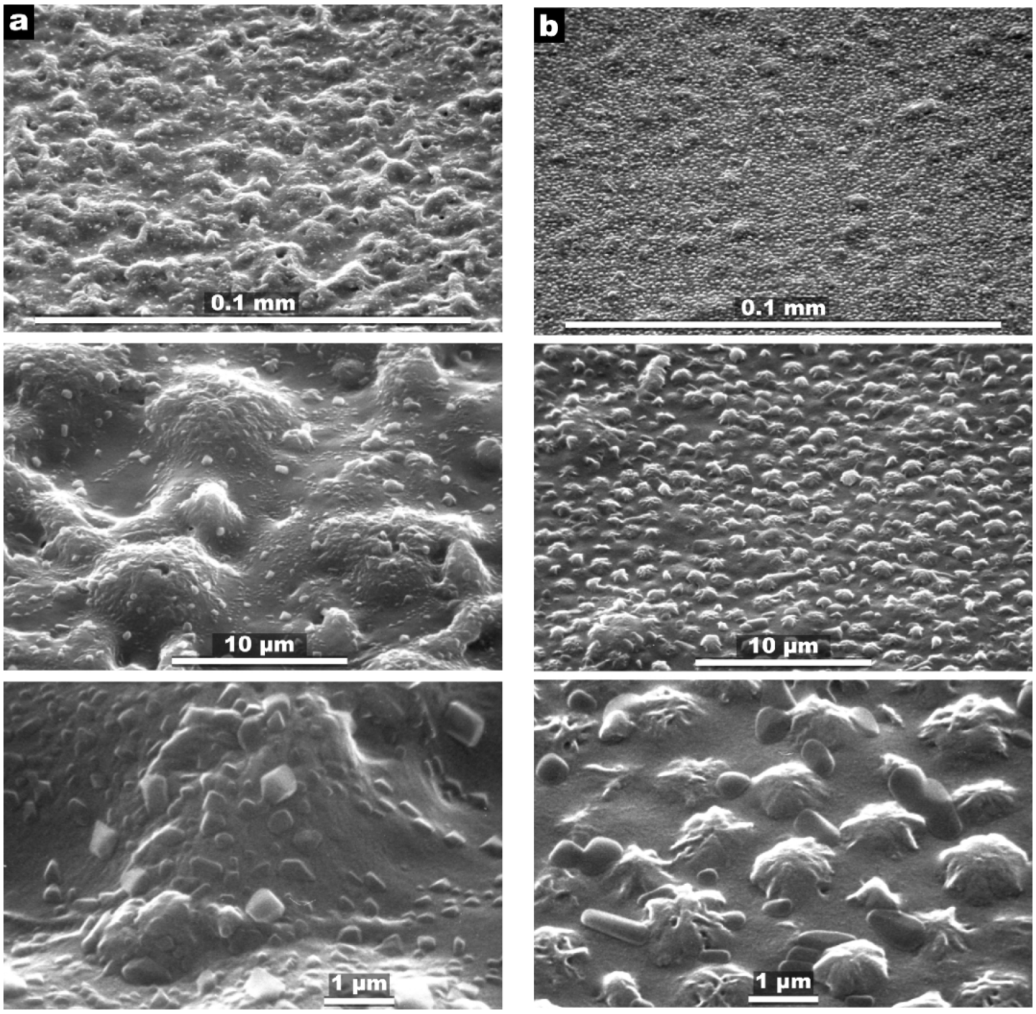

Fig. 9. SEM of etched polyurethane specimens at three magnifications: (a) 4: $PU_{C1\ PTHF}$ (b) 5: $PU_{C2\ PTHF}$ (c) 6: $PU_{C3\ PTHF}$ (d) 9: $PU_{D\ PTHF}$ (e) 10: $PU_{M\ PTHF}$.

studied, as it would require transmission electron microscopy to give appropriate resolution, and such examination would be better if a suitable chemical etching technique were available to reveal the bulk of the material and remove features associated with the surface.

Several chemical etching techniques were tried on these materials. Those based on alkaline reagents (whether potassium hydroxide in alkaline solution, or sodium ethoxide in ethanol) did not react enough even to completely remove the smallest spurious features associated with the moulded surfaces. On the other hand, the permanganic reagent with phosphoric acid gave smooth and uniform attack over all the materials. In Fig. 9, etched surfaces of all five materials are shown at three magnifications for easy comparison. $PU_{C1\ PTHF}$ (Fig. 9(a)) shows roundish regions which are raised and therefore more resistant to the etchant, surrounded by a flattish matrix. The scale of these regions is much larger than the length of hard and soft segments, so it appears as if some precipitation of one region has occurred during the reaction: in this case the precipitated part is more resistant to etching. The whole surface appears to be strewn with small objects between 0.2 and 0.8 μm in size, which look like crystals whose edges have been rounded off by partial dissolution. It may be that these are a particular chemical species, which has been released by the attack. $PU_{C2\ PTHF}$ (Fig. 9(b)) shows a similar structure, except that the resistant regions are much smaller, although they occupy about the same percentage of the total area. In $PU_{C3\ PTHF}$ and $PU_{M\ PTHF}$ (Figs. 9(c) and (e)), it appears that the relatively resistant material is in the majority, with non-resistant pockets being eaten out by the etchant. It may be that these pockets represent material precipitated during polymerization. In $PU_{D\ PTHF}$ (Fig. 9(d)) the overall etched texture is much flatter, so it would seem that the regions of chemical segregation are more or less equally attacked, although what structure there is seems to show a pattern similar to Figs. 9(c) and (e). Only $PU_{D\ PTHF}$ in Fig. 9(d) does not show the precipitated crystals: this is the only one of the

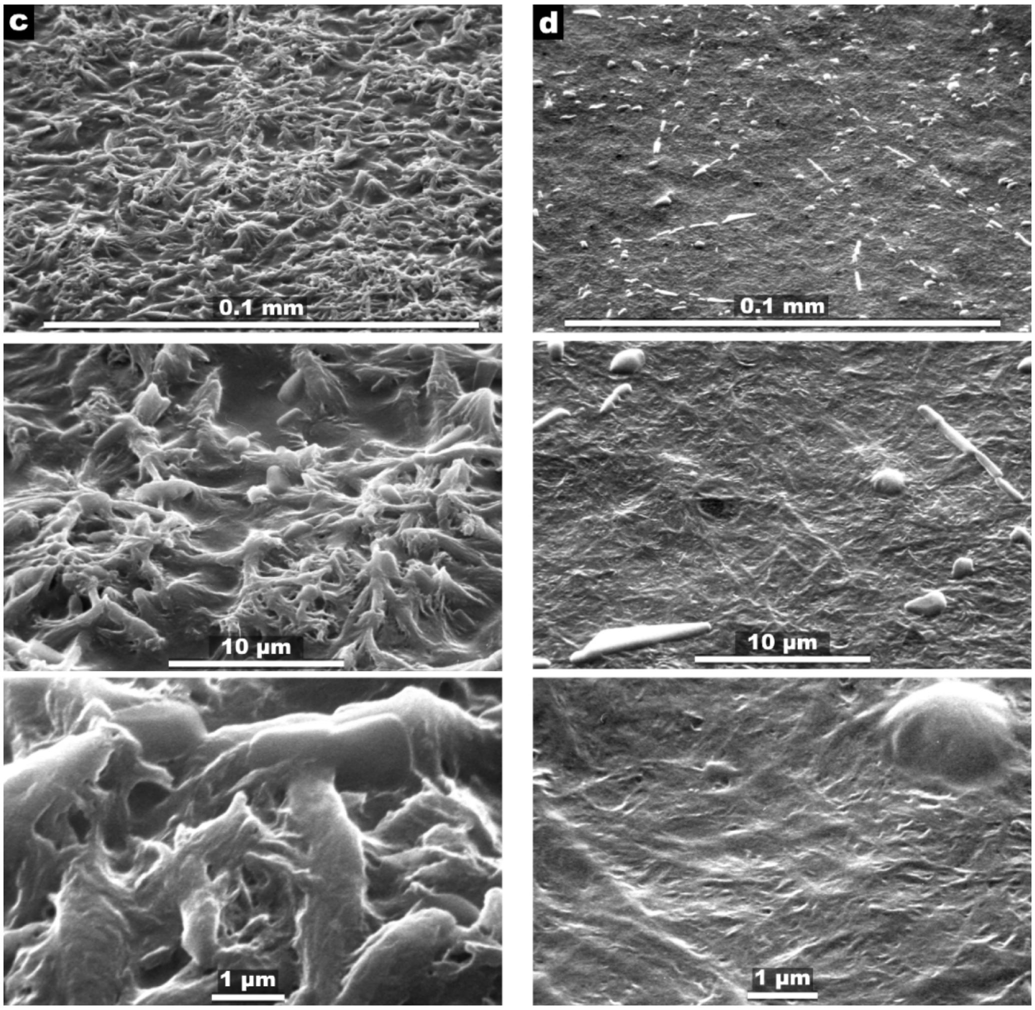

Fig. 9 (*continued*)

Table 3
Strain and recovered energy during the first and second loading–unloading

Type of PU structureand moles		E_{1C} (MPa cm)	E_{2C}[a] (%)	E_{1R}[a] (%)	E^0_{2R} (%)
PU$_{C1\ PEA}$ EG$_{51,4}$–PEA–(DBDI–MDI) (2.64:1:2:2)	I	40.1	55.3	15.72	15.74
	A	32.2	55.1	14.17	15.11
PU$_{C2\ PEA}$EG$_{51,4}$–(PEA–DBDI)–MDI (2.64:1:2:2)	I	37.0	58.6	18.3	19.9
	A	23.25	65.1	16.0	17.3
PU$_{C3\ PEA}$EG$_{51,4}$–(PEA–MDI)–DBDI (2.64:1:2:2)	I	41.3	51.0	13.8	13.8
	A	32.5	47.3	11.3	12.3
PU$_{C1\ PTHF}$ EG$_{51,4}$–PTHF–(DBDI–MDI) (2.64:1:2:2)	I	Not resistant at a 300% strain level			
	A	30.5	52.4	15.3	16.7
PU$_{C2\ PTHF}$ EG$_{51,4}$–(PTHF–DBDI)–MDI (2.64:1:2:2)	I	Not resistant at a 300% strain level			
	A	27.0	52.9	13.8	16.0
PU$_{C3\ PTHF}$ EG$_{51,4}$–(PTHF–MDI)–DBDI (2.64:1:2:2)	I	Not resistant at a 300% strain level			
	A	36.11	39.79	11.32	11.88
PU$_{D\ PEA}$EG$_{52,8}$–PEA–DBDI (2.64:1:4)	I	46.6	40.9	11.5	12.2
PU$_{M\ PEA}$EG$_{50}$ + PEA + MDI2.64 1 4	I	30.4	64.6	17.6	20.1
PU$_{D\ PTHF}$EG$_{52,8}$ + PTHF + DBDI 2.64 1 4	I	41.1	36.2	10.2	10.8
PU$_{M\ PTHF}$EG$_{50}$ + PTHF + MDI2.64 1 4	I	Not resistant at a 300% strain level			

I—initially; A—after annealing at 160 °C for 30 min.

[a] In % relative to E_{1C}.

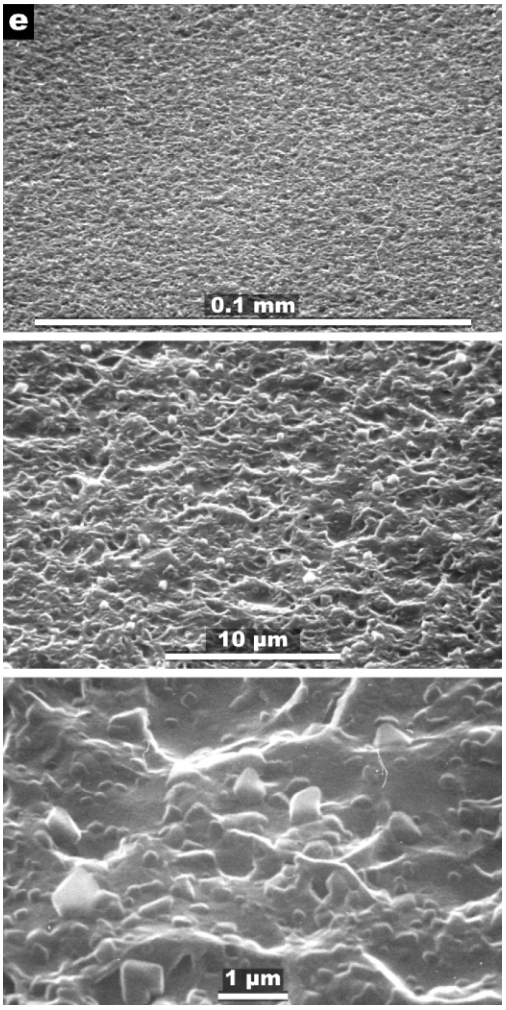

Fig. 9 (*continued*)

five examined by microscopy which does not contain MDI, so it may well be that the crystals are derived from units containing this monomer. At the highest magnification, there is only a faint suggestion of fine-scale structure such as seen in Fig. 8(f), which is most prominent in Fig. 9(b) (bottom). This particular etchant is therefore not ideally suited to distinguishing between the hard and soft segments.

3.5. Tensile strength properties

Stress–strain testing was performed on the initial polymer (Table 1) or on the same polymer after annealing for 30 min at 150, 160, 170 and 180 °C. Fig. 10 reveals noticeable differences in the mechanical performance of the different ordered copolyurethane elastomers.

Strong variations start to occur above 150 °C, and as noted from DSC results there is a good case for attributing this to variations in copolymeric order and a reduction in mesophase interactions (Fig. 10). As a rule the higher the disorder the better are the elastic properties of the elastomer. This fact is characterized by a lower variation of the Young's Modulus during the augmentation of deformation, and also by a lower residual elongation.

Similar conclusions can be obtained with regard to the general strain energy (mechanical yield) of polymer (E_{1C}) (intermolecular cohesion) measured during 0–300% elongations (Table 3). These conclusions should be correlated with the elastic properties reflected by the degree of the maintenance of the mechanical yield during the second loading (Table 3). Thus, in the case of $PU_{C1\ PEA}$ type, the strain energy of the elastomer network E_{1C} of 40.1 MPa cm (Table 3) becomes higher than in the case of the MDI-PEA based PU, e.g. $PU_{M\ PEA}$ (30.4 MPa.cm) reflected also by the increase of hardness from 92 to 98° Sh A, as well as by the augmentation of the 100 and 300% tensile stresses from 8.1 to 11.4 MPa and from 22.0 to 25.3 MPa, respectively, and also by the enhance of the strength stress from 47.0 to 48.7 MPa. Simultaneously the residual elongation at break decreases from 35 to 20%.

It is worth mentioning that other further subsequent deformation cycles follow in general the same pathway as the second hysteresis cycle. Due to this situation it is

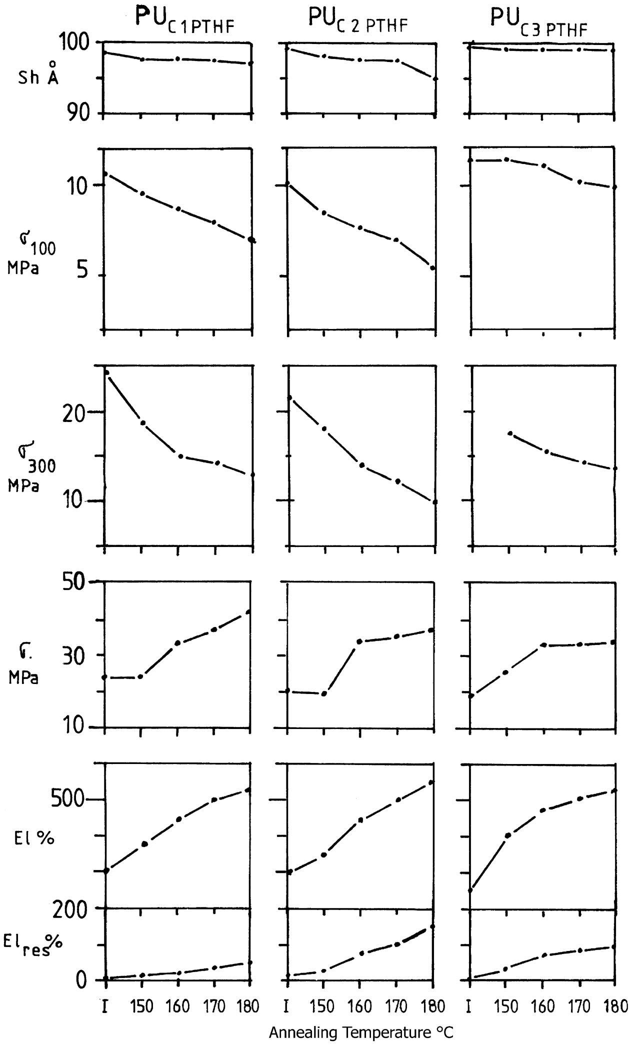

Fig. 10. Influence of the annealing on the mechanical properties of PTHF-based copolyurethanes: Initially (I) and after annealing for 30 min at 150, 160, 170 and 180 °C.

assumed that the major suprastructural transformation appears during the first loading similar as described in other cases [15]. It should be mentioned that elastomers like $PU_{C1\ PTHF}$, $PU_{C2\ PTHF}$ and $PU_{C3\ PTHF}$ which normally exhibit relatively low ultimate tensile strength stresses can be noticeably improved on employing an annealing process preferably performed at 160 °C for 30 min in inert atmosphere, when any other eventual parallel process of degradation does not practically exist.

3.6. PU Thermomechanical behaviour

The effect of ordering in the copolyurethane elastomers was also assessed on employing the thermomechanical analyses with the aid of a home-made thermal creep testing machine of own design and construction [11], which follows the course of elongation under constant load of a pre-tensioned sample so to start from a constant initial 50% strain level.

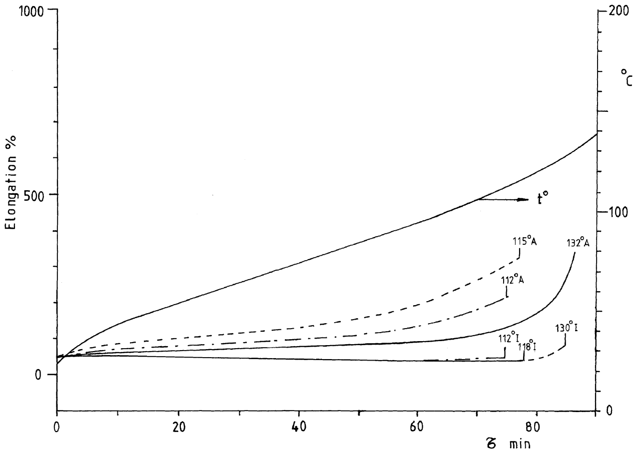

Fig. 11. Thermomechanical curves of copolyurethanes with PTHF: (—)-$PU_{C1\ PTHF}$; (- - -)-$PU_{C2\ PTHF}$; (– -)-$PU_{C3\ PTHF}$; (I)-initially; (A)-after annealing.

The variation of elongation under the constant characteristic initial 50% strain load was followed on employing a constant temperature increase increment of about 1 °C/min. The results which are portrayed in Figs. 11 and 12 show the dependence of thermomechanical properties on the sequential ordering of the block copolyurethane blocks.

As seen in Fig. 11 in the case of PU based on PTHF soft segments, the course of the thermal creep curves achieved on original PU as obtained after synthesis does not depend essentially on the sequential block ordering. All of these polymers, $PU_{C1\ PTHF}$, $PU_{C2\ PTHF}$ and $PU_{C3\ PTHF}$ keep their elasticity modulus very well on heating. Differences only appear with regard to the temperature at which rupture in the polymer occurs. Thus, $PU_{C2\ PTHF}$ characterized by the presence of accumulated EG–MDI blocks (EM) display a higher resistance at temperatures situated around 130 °C, whereas in the case of $PU_{C3\ PTHF}$ where the EG–DBDI blocks are preponderant the temperature of break decreases to 112 °C.

After annealing of these polymers at 160 °C for 30 min, the thermomechanical properties change and the elongation

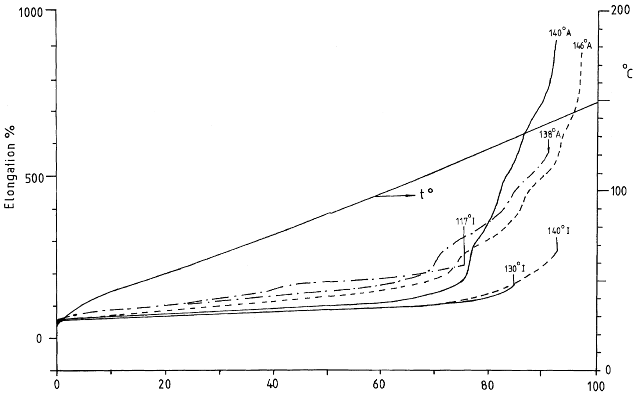

Fig. 12. Thermomechanical curves of copolyurethanes with PEA: (—)-$PU_{C1\ PEA}$; (- - -)-$PU_{C2\ PEA}$; (– -)-$PU_{C3\ PEA}$; (I)-initially; (A)-after annealing.

of the polymer specimen increases noticeably along with the temperature augmentation. The higher deformation in dependence of temperature is remarked in the case of $PU_{C2\ PTHF}$ whereas the most stable annealed PU is $PU_{C1\ PTHF}$, which possesses a statistical distribution of the EG–MDI and EG–DBDI blocks.

A similar situation is observed with the PU based on PEA segments (Fig. 12). The enhanced accumulation of EG–MDI blocks ($PU_{C2\ PEA}$) induces a higher resistance to heating with $T_{break} = 140\ ^\circ C$ whereas in the case of $PU_{C3\ PEA}$ with preponderant EG–DBDI block accumulations, T_{break} decreases to 117 °C. In this case should be mentioned also the more pronounced enhancement of elongation against temperature. As shown in Fig. 12, a significant difference in the thermomechanical curves appears in the case of the annealed PU at 160 °C for 30 min when all the break temperatures increase. The elongation increment increases significantly too with the augmentation of temperature. A higher degree of elongation versus temperature is ascertained in the case of $PU_{C3\ PEA}$ with accumulated EG–DBDI hard segments. It should be also mentioned that the annealing of $PU_{C3\ PEA}$ improves its properties from all points of view. So, the temperature at break increases from 117 to 138 °C, in parallel with a lower dependence of deformation against temperature.

4. Conclusions

When performing elastomeric PU synthesis in which two diisocyanates are used, one being MDI with a rigid bend molecule and DBDI with a variable molecular geometry allowing an almost linear conformation, DBDI leads to hard segment associations reflected by significant crystallinity.

Significant changes are brought about by changing the order of introduction of the two diisocyanates.

The polyurethanes with DBDI only (PU_D types) show the highest tensile stress at 100% and maintain this value almost unchanged up to 300%, while in the same elongation range those with MDI only (PU_M types) start with a low tensile stress which increases. The highest ultimate strength stresses, however, were obtained when the two diisocyanates were introduced simultaneously in the prepolymer synthesis stage (PU_{C1} types). This eliminates the major inconvenience derived from the high permanent deformability e.g. residual elongations of 155–160%, and leads also to a significant decrease of the crystallinity otherwise undesired for an elastomer. With the PU_{C1} types especially the greater strength stress given by DBDI is combined with the elastic recovery of a more conventional polyurethane. Other augmented mechanical properties achieved with DBDI (hardness, tear strength and strain energy) are also retained in the polymers with mixed isocyanates. Therefore with mixture the general advantages of DBDI are retained while eliminating the one undesirable effect.

Thus the desired augmention in properties can best be achieved by only using a half quantity of the speciality DBDI along with the cheaper generally available MDI.

When PTHF was used as macrodiol the best mechanical properties were achieved only after an additional annealing performed by heating the PU samples at 160 °C for 30 min. The changes induced by annealing in the intermolecular structure in the mesophase interaction could only be evidenced in the DSC measurements and thermomechanical curves. In contrast, the general X-ray diffractograms regarding the hard segment self association do not present major changes in the polymer crystallinity after annealing at 160 °C for 30 min ($PU_{C1\ PEA}$ and $PU_{C2\ PEA}$).

References

[1] Cocea E, Caraculacu A, Marculescu Cr, Petrus A, Matei I. Studii si Cercetari Stiintifice Chimice- Acad Romana-Filiala Iasi 1959;X:2261.
[2] Lyman DJ, Heller J, Bartlow M. Die Makromol Chem 1965;84:64.
[3] Oertel G. Polyurethane Handbook. Munich: Hanser Publishers; 1985. p. 570.
[4] Matei I, Cocea E, Caraculacu A, Petrus A, Polyurethane handbook, vol. Xiii(1). Munich: Hanser Publishers; 1962. p. 109.
[5] Caraculacu A, Caraculacu G. J Macromol Sci-Chem 1985;A22(5–7): 631.
[6] Gowerr LA, Wang TLD, Lyman DJ. J Biomater Sci Polymetr Ed 1994;6(8):761.
[7] Prisacariu Cr, Agherghinei I. J Macromol Sci Pure Appl Chem 2000; A37(7):785.
[8] Olley RH, Bassett DC, Blundell D. J Polymer 1986;27:344–8.
[9] Aboulfaraj M, Ulrich B, Dahoun A, G'Sell C. Polymer 1993;34(23): 4817.
[10] Martin C. PhD Thesis, Keele University, UK, 2000.
[11] Prisacariu, Cr. Polytechnical Inst Gh Asachi, Bull Iasi 2001; XLVII, (LI)1-2, Section I. Mathematics, Theoretical Mechanics, Physics.
[12] Caraculacu A, Agherghinei I, Gaspar M, Prisacariu Cr. J Chem Soc Perkin Trans 2 1990;1343.
[13] Caraculacu A, Agherghinei I, Baron P, Coseri S. Rev Roumain Chim 1996;41(7–8):539.
[14] Park CG, Tasumi M. J Phys Chem 1991;95(7):2757.
[15] Prisacariu Cr. Doctorate Thesis, Gh Asachi University, Iasi, Romania, June, 1998.